

Visualized Blow-off from Helium Irradiated Tungsten in Response to ELM-like Heat Load^{*})

Shin KAJITA, Noriyasu OHNO¹⁾, Wataru SAKAGUCHI¹⁾ and Makoto TAKAGI¹⁾

EcoTopia Science Institute, Nagoya University, Furo-cho, Chikusa, Nagoya 464-8603, Japan

¹⁾*Graduate School of Engineering, Nagoya University, Nagoya 464-8603, Japan*

(Received 28 November 2008 / Accepted 25 December 2008)

Laser-induced blow-off from a tungsten surface that was exposed to helium plasma is investigated experimentally in the divertor simulator NAGDIS-II. The pulse width of the laser is submillisecond and is similar to the duration of type-I edge localized modes in ITER. The temporal evolution of blow-off particles, which are visualized by the electron impact excitation in the surrounding plasma, is investigated by using filter spectroscopy. We demonstrate the effect of helium irradiation damages on the tungsten ejection behavior in response to a transient heat load.

© 2009 The Japan Society of Plasma Science and Nuclear Fusion Research

Keywords: NAGDIS-II, helium irradiation, tungsten, transient heat load

DOI: 10.1585/pfr.4.004

1. Introduction

In ITER, tungsten is a candidate material for the divertor plate and the first wall. This is because tungsten has good thermophysical properties, a high melting point, a low sputtering rate, and a low tritium inventory. Moreover, tungsten is assumed to be an in-vessel mirror material because it has a rather good optical reflectivity in a wide wavelength range [1]. It is known that helium bombardment leads to helium-induced damages accompanying microstructural evolution, such as dislocation loops, helium holes/bubbles [2], and fiberform nanostructures [3]. Since helium is produced by a nuclear fusion reaction, it is necessary to take into account the effect of helium bombardment in future fusion plants. The helium irradiation damages could result in decreases in the optical reflectivity [4] and in the thermal conductivity near the surface [5], and additionally, an increase in the hydrogen retention [6]. An important issue concerning the helium irradiation damages is the change in the effects of the transient heat load accompanied by ELMs (edge localized modes) and disruptions on the material.

From the laser irradiation experiments, it has been revealed that, when using a short nanosecond laser pulse, the surface roughness is significantly enhanced [7] and the threshold laser pulse energies for melting and ablation decrease because of submicrometer-sized bubbles [8, 9]. In contrast, in the case of a long submillisecond laser pulse, the pulse width of which corresponds to the duration of typical type-I ELMs in ITER, it has been found that the surface roughness decreases [10], and the optical reflectivity considerably recovers because of the decrease in the

surface roughness [4]. Moreover, in the case of a fiberform nanostructure, it is interesting to note that the structure easily melts and is destroyed even when irradiated with a weak laser pulse [11]. This is because the effective thermal conductivity is decreased significantly by the fine structure [5]. Although the modification of the surface nature has been discussed on the basis of the experiments, the impurity release from the material in response to a transient heat load like ELMs has not been investigated as yet. Since the mass loss or quantity of the injected impurity in response to transient heat load affects the lifetime of the material and the performance of the core plasma, it is important to investigate the characteristics of impurity ejection from a helium-irradiated surface.

In this study, we investigate the effects of a transient heat load on a helium-irradiated surface by using submillisecond laser pulses in a linear plasma device. Since the laser pulses are injected while the target material is exposed to the plasma, a laser-induced blow-off is visualized by the surrounding plasma, that is by the electron impact excitation followed by the emission, which can be detected by using a fast camera. From a comparison of the emission of tungsten neutral WI in response to the transient heat load, we will discuss how the damages caused by the helium irradiation affect the impurity release from the material.

2. Experimental Setup and Calculation

Experiments were performed in the linear divertor plasma simulator NAGDIS (NAGoya DIvertor Simulator)-II [12, 13]. Figure 1 shows the schematic representation of the cross section of the experimental setup. Helium

author's e-mail: kajita@ees.nagoya-u.ac.jp

^{*}) This article is based on the invited talk at the 25th JSPF Annual Meeting (2008, Utsunomiya).

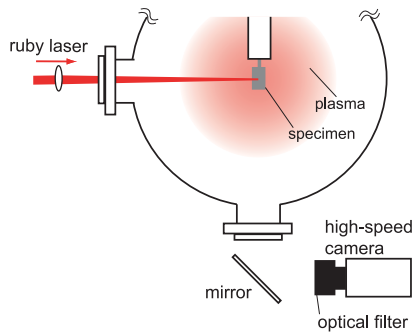


Fig. 1 Schematic representation of the experimental setup in the divertor simulator NAGDIS-II. The emission of the ejected particles from the specimen in response to the laser pulse is observed by high-speed camera.

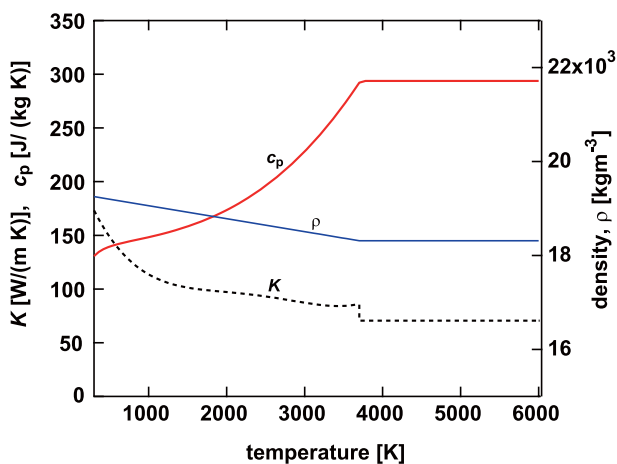


Fig. 2 Temperature dependences of the thermal conductivity, specific heat, and density used in the calculation.

or deuterium plasma was produced in the source region by dc arc discharge, and a specimen was exposed to the plasma in the downstream test region, as shown in Fig. 1. The electron density and the electron temperature in the helium plasma were $2 \times 10^{19} \text{ m}^{-3}$ and 6 eV, and those in the deuterium plasma were $2 \times 10^{18} \text{ m}^{-3}$ and 6 eV. Powder metallurgy tungsten with a thickness of 0.2 mm was used as the specimen. Ruby laser pulses were injected to the vacuum vessel through a viewing port. The pulse width was approximately 0.6 ms, and the pulse energy was $< 5 \text{ J}$. By focusing the beam with a lens, the pulse energy per unit area was controlled up to several MJm^{-2} at the specimen. The emission from the ejected tungsten neutral particles ($\lambda = 400.9 \text{ nm}$) was detected with an image-intensified CCD (charge coupled device) camera (Photoron: FASTCAM-MAX 120K I2) through a narrow band-pass optical filter. The frame rate was 30 000 fps (frames per second) in the experiments. The surface temperature was measured by using a radiation pyrometer.

The temporal evolution of the material temperature in

response to the laser pulse was calculated numerically by solving a heat conduction equation. The details of the numerical method can be found in Refs. [5, 14]. As shown in Fig. 2, temperature dependences of the thermophysical properties were taken into account. As for the thermal conductivity and specific heat, the data in Ref. [15] were used, and for density, we extrapolated the data in Ref. [16] to the melting point. Moreover, it is known that optical reflectivity decreases with temperature; therefore, this effect was also taken into account on the basis of experimentally obtained value [17].

3. Results and Discussion

3.1 Temporal evolution of emission

Irradiation experiments were performed under three different experimental conditions, cases (i)-(iii). Deuterium plasma was used in case (i), while helium plasma was used in cases (ii) and (iii). The incident ion energy for cases (i)-(iii) were 40 eV, 15 eV, and 50 eV, respectively, and the surface temperatures for cases (i), (ii), and (iii) were 1200 K, 1730 K, and 1780 K, respectively. In the deuterium plasma, because the surface temperature was considerably high, blistering did not occur. Thus, there was no change in the surface morphology in case (i), while damages due to helium irradiation were observed in cases (ii) and (iii).

In Fig. 3, images show the tungsten emission profiles in response to the laser pulse. Figures 3 (a)-(a''), (b)-(b''), and (c)-(c'') correspond to cases (i), (ii), and (iii), respectively. The temporal evolutions of the emission intensity in the three cases are shown in Figs. 3 (d), (e), and (f), respectively. The emission intensity was obtained by integrating the CCD count in the emission area, approximately $15 \text{ mm} \times 15 \text{ mm}$ in front of the laser-irradiated side of the plate. Because of the exposure to the helium plasma, helium holes/bubbles are formed in case (ii), and fiberform nanostructure is formed in case (iii), as shown in Figs. 3 (e) and (f). It is suggested that the main emission originates from the electron impact excitation of the ejected tungsten neutrals by the surrounding plasma. The laser ablation process that produces high-density plasma did not take place because the laser power in the experiments was $\sim 10^9 \text{ Wm}^{-2}$, which was sufficiently lower than the typical required laser power for ablation of $> 10^{13} \text{ Wm}^{-2}$ [18]. In case (i), the emission region is smaller than those in cases (ii) and (iii). This could be attributed to the facts that the plasma density in the deuterium plasma was an order of magnitude lower than that in the helium plasma and that the tungsten emission could be enhanced by the helium irradiation in cases (ii) and (iii). Further discussion about the differences among the three cases is provided later.

It is interesting to note that temporal evolution of emission intensity has a peak around 0.1-0.2 ms in case (iii), whereas the peak in case (i) is at approximately 0.3 ms. Figure 4 shows the calculated temporal evolutions

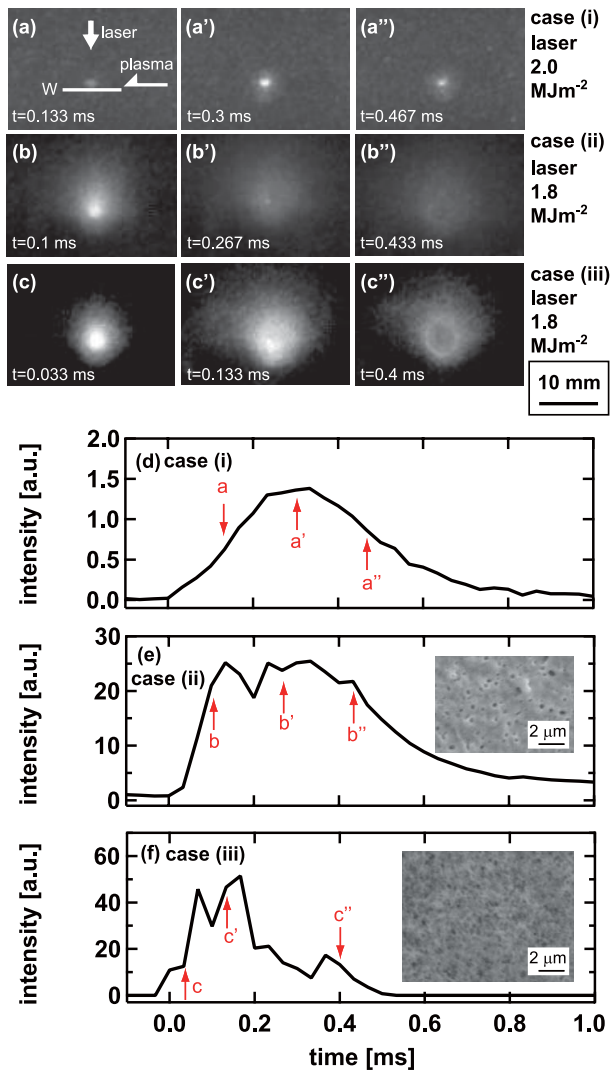


Fig. 3 Images of tungsten neutral emission profiles at different times (a)-(a'') in case (i), (b)-(b'') in case (ii), and (c)-(c'') in case (iii). (d), (e), and (f) show the temporal evolutions of the emission intensity in cases (i), (ii), and (iii), respectively.

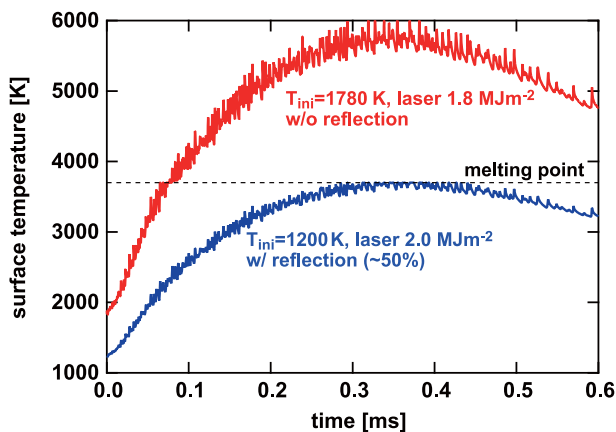


Fig. 4 Calculated surface temperature evolution in response to the laser pulse irradiation under two different conditions.

of the surface temperature. For case (i), the reflection of the laser beam, which was typically 50%, was taken into account, but, for case (iii), it was assumed that all the energy was deposited on the surface because the surface reflectivity became almost zero. The fiberform nanostructure had so complicated structure that the photons that entered the surface were not reflected back. The calculated surface temperature had a peak at approximately 0.3-0.4 ms, which was consistent with the observed temporal evolution of the emission intensity in deuterium plasma of Fig. 3 (d). In case (iii), on the other hand, the emission intensity is not consistent with the temporal evolution of the calculated temperature. Since the fiberform nanostructure would drastically decrease the thermal conductivity near the surface, an anomalous temperature increase could take place [5] in case (iii). However, even if such effects were taken into account in the calculation, it was difficult to obtain a result that had a temperature peak at approximately 0.1-0.2 ms. We suspected that the fiberform structure was anomalously heated even in the earlier phase. The anomalous heating would destruct the fine structure, and a part of the heat might be used for the sublimation process, which consumed considerable heat; consequently, the emission decreased from at approximately 0.3 ms even if the laser power was almost maximum at that time. In case (ii), the emission duration was longer than that in cases (i) and (iii), as shown in Fig. 3 (e). It was speculated that the bursting of helium bubbles would take place and result in some tungsten droplets [9] even after the laser irradiation. Because the helium bubbles could burst even if the temperature was lower than the melting point [8], the bursting of bubbles could take place while the laser heat was conducted toward radially in an outward direction from the laser-irradiated area.

3.2 Pulse energy dependence

Figures 5 (a), (b), and (c) show the laser pulse energy dependences of the emission intensity in cases (i), (ii), and (iii), respectively. In cases (ii) and (iii), the specimen was exposed to the helium plasma before the laser irradiation for 1200 and 4900 s, respectively. The relative optical reflectivity against the initial value, which was measured by using a He-Ne laser [4], decreased because of the plasma irradiation to 34% in case (ii), and to almost 0% in case (iii). The laser pulse energy was gradually increased to approximately 2.0 MJm⁻². In case (iii), we irradiated the laser pulse after the relative reflectivity decreased to less than 0.1 because of the helium plasma exposure. The time interval between the laser pulses was several minutes. In case (ii), the time interval between the laser pulses was approximately 5 min. Thus, since the time interval was shorter than the time required to form the micrometer-sized helium bubbles in case (ii), it should be noted that the surface condition could be changed between laser pulses. In case (i), intensity gradually increased from approximately

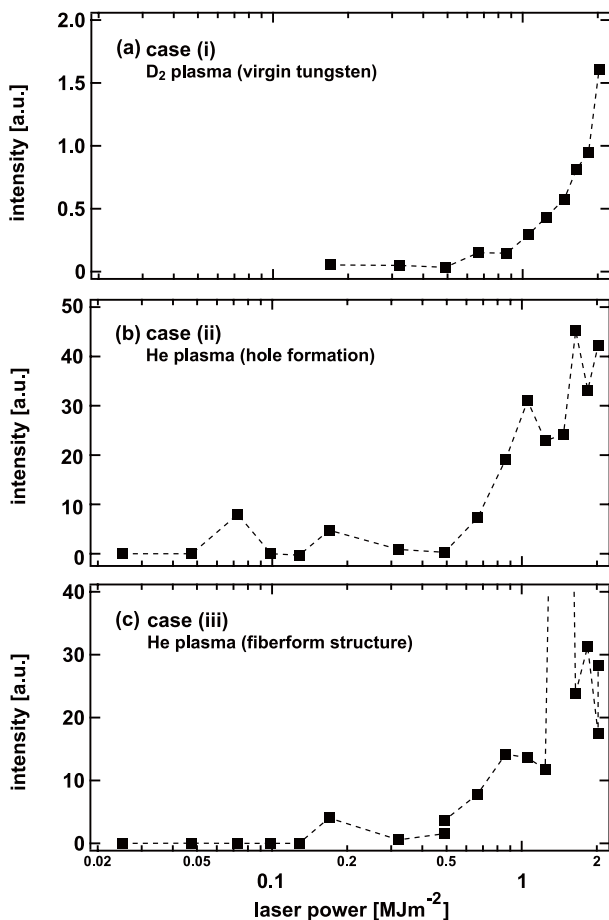


Fig. 5 Laser pulse energy dependences of the emission intensity in cases (i)-(iii). The pulse energy was gradually increased to approximately 2 MJm^{-2} .

1 MJm^{-2} . In cases (ii) and (iii), it seemed that the intensity increased from a slightly lower pulse energy, typically 0.5 MJm^{-2} . Moreover, emission was observed at a considerably lower pulse energy: 70 kJm^{-2} and 150 kJm^{-2} for case (ii) and 150 kJm^{-2} for case (iii). We believe that the damage due to helium irradiation decreases the onset pulse energy of the emission. In case (ii), the surface contains submicrometer-sized holes. Thus, it is possible that the bursting of these bubbles decrease the threshold laser pulse energy. In case (iii), the anomalous increase in the temperature of the fiberform structure could lead to the reduction in the threshold pulse energy. In the experiment, the laser pulses irradiated to the same position of the specimen. The helium irradiation damage could be recovered by the laser irradiation; moreover, the damage could be formed in between the laser pulse irradiation because the sample was exposed to the helium plasma. Thus, we should say that the surface nature was different for each laser pulse irradiation. If the surface roughness decreased because of the laser irradiation, the emission intensity might decrease at the next irradiation. Consequently, it was thought that pulse-by-pulse difference in the emission intensity increased. In

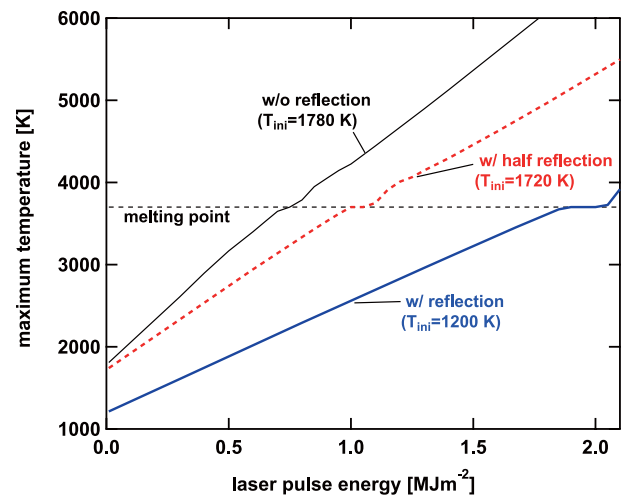


Fig. 6 Laser pulse energy dependences of the calculated maximum surface temperature in three different cases.

Fig. 5 (c), the intensity at 1.5 MJm^{-2} was extraordinarily larger than the others. This was because arcing was initiated in response to the laser pulse and this increased the emission intensity anomalously. It was found that the fiberform nanostructure made it significantly easier to initiate arcing [19].

The pulse energy dependence of the emission did not change considerably in cases (ii) and (iii) except for during arcing, although we had assumed that the fiberform structure could significantly decrease the threshold pulse energy for the emission in these cases as compared to the case with bubbles. Indeed, the modification of the surface nature and the local temperature response were considerably different in the case of the fiberform structure and that of a surface with bubbles [5]. However, with respect to the emission, that is, the ejection of material, the bursting of hole, which could take place even if the surface temperature was considerably lower than the melting point, could increase the emission by forming microdroplets. Therefore, we should say that it was not easy to conclude the differences between the two cases regarding with the impurity ejection, although we could say that the damages due to helium irradiation enhance the ejection in both the cases.

Figure 6 shows the calculated maximum temperature as a function of the laser pulse energy in three different cases. We used the surface temperatures of 1200 K, 1720 K, and 1780 K, which corresponded to the cases (i)-(iii). The optical reflectivity for a clean surface was used in case (i), whereas half of this reflectivity was used in case (ii), and no reflection was assumed in case (iii). We should say that the optical reflectivity in the actual situation was an unknown factor, and it could change while the laser was irradiated because of a change in the morphology, as shown in Ref. [4]. However, the calculation with the above assumptions in the reflectivity can provide us

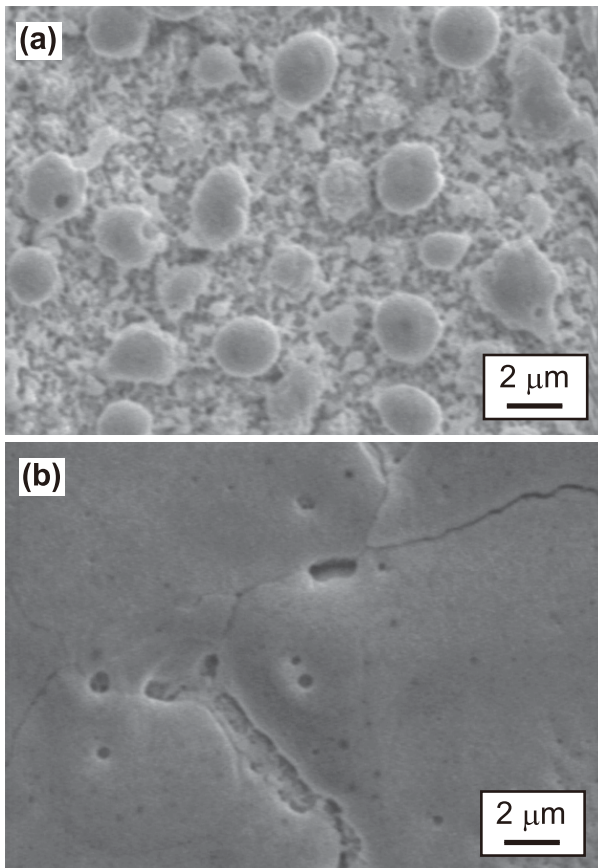


Fig. 7 SEM micrographs after the series of laser pulse irradiations in case (iii). (a) shows the peripheral region of the laser beam, and (b) shows the central region of the laser.

with a benchmark for temperature change, which is useful for understanding the phenomena in response to laser pulse irradiation. In cases (ii) and (iii), the onset laser pulse energy required for observing the emission was slightly less than the melting threshold energy but close to the value. As previously discussed, it was understandable in cases (ii) and (iii) that the emission was observed from a lower pulse energy than the melting threshold. In contrast, the calculations predicted that the melting threshold in case (i) might exist at approximately 1.8 MJm^{-2} , which was slightly larger than the observation threshold of approximately 1 MJm^{-2} . In general, in order to enhance the emission, increases of tungsten neutral density and/or electron density are necessary. In case (i), as discussed in the previous section, the emission intensity agreed well with the temperature response. When the surface temperature is increased, tungsten neutral release is enhanced; moreover, thermionic electron emission is initiated. We speculate that the emission in case (i) is mainly due to the electron excitation by the electrons produced by thermionic emission. Indeed, in case (i), the emission area was significantly smaller than the area in cases (ii) and (iii), as shown in Figs. 3 (a)-(c). As a future work, it will be interesting to

conduct the experiments in a higher pulse energy range in which laser-induced vaporization would take place. If the intensity in case (i) significantly increased in the higher pulse energy range, the signal in Fig. 5 (a) would be a precursor signal before the real blow-off signal.

Figure 7 shows the SEM micrographs after the series of laser pulse irradiations in case (iii). Figure 7 (a) corresponds to the peripheral region, where the laser pulse energy was lower than that in the central region shown in Fig. 7 (b). At the peripheral region, micrometer-sized balls were formed probably in the process of the melting of the fiberform structure. It was reported that a $1.5 \mu\text{m}$ tungsten ball was formed on a microcone array by laser pulse irradiation to tungsten in a helium atmosphere [20]. It is of interest to point out that the size of the ball in our case is similar to that given in Ref. [20], although the formation mechanism may be different. It is indicated that such a ball can be produced by a pulsed heat load if the fiberform structure is formed on the surface. It is important to note that the micrometer-sized balls can be high- Z dust particles, which are destructive for the core plasma, if they are released from the surface. In the central region, the surface melted completely, and many cracks could be observed. The formation of a rough surface might be attributed to the fact that the laser pulse energy was gradually increased from the lower energy in the experiment. Since the fiberform structure could easily be destroyed and form balls even at a low pulse energy, as shown in Fig. 7 (a), the surface might retain the irradiation history. That is, if micrometer-sized balls were formed on the surface, it might be difficult to completely modify the micrometer-sized structure, which was considerably larger than the fiberform structure, even if the laser pulse energy was greater; and, consequently, a rough surface might be formed after the series of laser pulse irradiation.

4. Summary

The effects of ELM-like transient heat load to the tungsten exposed to helium plasma were investigated by using a submillisecond pulsed laser. The ejected tungsten particles in response to the laser pulses were detected by fast CCD camera. When the laser pulse energy was greater than 0.5 MJm^{-2} , clear WI emission was observed from the helium-irradiated surface. The emission could be observed at a considerably lower pulse energy sometimes, although such an emission was not observed from the surface without damages due to helium irradiation when the laser pulse energy was lower than 1 MJm^{-2} . Two processes were proposed for the mechanisms that could cause the tungsten ejection from the low pulse energy. One was the bursting of bubbles, which could produce tungsten microdroplets, and the other was the anomalous temperature increase in the fiberform nanostructure. The results suggested that the damages due to helium-irradiation, that is, bubbles/holes and the fiberform structure, could enhance the tungsten im-

purity release from the material in response to the transient heat load like ELMs in future fusion devices. The formation of a micrometer-sized ball was observed in a region where weak laser pulses irradiated the fiberform nanostructure. Since the ball formation could enhance the high-Z dust particles in fusion devices, it is important to investigate the formation mechanism, which will be dealt with in a future work.

Acknowledgments

This work was supported in part by a Grant-in-Aid for Young Scientists (Start-up) (No. 19860096) from the Japan Society for the Promotion of Science (JSPS).

- [1] D.V. Orlinski, V.S. Voitsenya and K.Y. Vukolov, *Plasma Devices and Operations* **15**, 33 (2007).
- [2] H. Iwakiri, K. Yasunaga, K. Morishita and N. Yoshida, *J. Nucl. Mater.* **283-287**, 1134 (2000).
- [3] S. Takamura, N. Ohno, D. Nishijima and S. Kajita, *Plasma Fusion Res.* **1**, 051 (2006).
- [4] W. Sakaguchi, S. Kajita, N. Ohno and M. Takagi, to be published in *Journal of Nuclear Materials*.
- [5] S. Kajita, S. Takamura, N. Ohno, D. Nishijima, H. Iwakiri and N. Yoshida, *Nucl. Fusion* **47**, 1358 (2007).
- [6] M. Tokitani, M. Miyamoto, K. Tokunaga, T. Fujiwara, N. Yoshida, S. Masuzaki, N. Ashikawa, T. Morisaki, M. Shoji, A. Komori, LHD Experimental Group, S. Nagata and B. Tsuchiya, *J. Nucl. Mater.* **363-365**, 443 (2007).
- [7] S. Kajita, D. Nishijima, N. Ohno and S. Takamura, *J. Plasma Fusion Res.* **81**, 745 (2005).
- [8] S. Kajita, D. Nishijima, N. Ohno and S. Takamura, *J. Appl. Phys.* **100**, 103304 (2006).
- [9] S. Kajita, N. Ohno, S. Takamura, W. Sakaguchi and D. Nishijima, *Appl. Phys. Lett.* **91**, 261501 (2007).
- [10] S. Kajita, S. Takamura, N. Ohno and T. Nishimoto, *Plasma Fusion Res.* **2**, 009 (2007).
- [11] N. Ohno, S. Kajita, D. Nishijima and S. Takamura, *J. Nucl. Mater.* **363-365**, 1153 (2007).
- [12] N. Ohno, N. Ezumi, S. Takamura, S.I. Krasheninnikov and A.Y. Pigarov, *Phys. Rev. Lett.* **81**, 818 (1998).
- [13] S. Takamura, N. Ohno, D. Nishijima and Y. Uesugi, *Plasma Sources Sci. Technol.* **11**, A42 (2002).
- [14] S. Kajita, T. Hatae and V.S. Voitsenya, *Plasma Fusion Res.* **3**, 032 (2008).
- [15] E. Koch-Bienemann, L. Berg and G. Czack, *Gmelin Handbook of Inorganic Chemistry (Tungsten)* 8th ed. (Springer, Berlin, 1989) Vol. Suppl. A3.
- [16] *Thermophysical properties of high temperature solid materials*, ed. by Y.S. Touloukian (Macmillan, New York, 1967).
- [17] V.S. Voitsenya, V.G. Konovalov, M.F. Becker, O. Motojima, K. Narihara and B. Schunke, *Rev. Sci. Instrum.* **70**, 2016 (1999).
- [18] J.F. Ready, *Effects of High-Power Laser Radiation* (Academic press, New York, London, 1971).
- [19] S. Kajita, S. Takamura and N. Ohno, "prompt ignition of unipolar arc on helium irradiated tungsten", *Nuclear Fusion* (in press).
- [20] Y. Kawakami and E. Ozawa, *Appl. Phys. A* **74**, 59 (2002).